

Elevation, Ice Thickness and Structure Map Maps of the Central Part of the Filchner-Ronne Ice Shelf

By Franz Thyssen*, Andreas Bombosch* and Henner Sandhäger*

Summary: Improved maps of surface elevation, total ice thickness and meteoric ice thickness have been plotted using digital data obtained by airborne electromagnetic reflection (EMR) sounding during the course of three expeditions to the central part of Filchner-Ronne Ice Shelf (FRIS). These data have also been used to map the shape and the thickness of an extensive layer of marine ice located below the meteoric ice and to classify structures within the ice shelf by their appearance in the EMR records. The aerial distribution of these structures has been plotted in a further map.

The correlation of the results shown in the different maps has helped to improve the understanding of the complex glaciological situation within the central part of FRIS. In addition, the extensive data net forms a reasonable base for further modelling work on a double-layered ice shelf.

Zusammenfassung: Die verbesserten Karten der Oberflächenhöhe, der Gesamteismächtigkeit und der meteorischen Eismächtigkeit wurden auf der Grundlage digitaler Daten erstellt, die in einem Zeitraum von drei Expeditionen in den zentralen Teil des Filchner-Ronne Schelfeises mit Hilfe von EMR-Flugmessungen (elektromagnetisches Reflexionsverfahren: EMR) gewonnen wurden. Die Daten sind ebenfalls dazu benutzt worden, die Form und die Mächtigkeit einer ausgedehnten marinen Eisschicht unterhalb des meteorischen Eises darzustellen und Strukturen innerhalb des Schelfeises nach ihrer Erscheinungsform in den EMR-Registrierungen zu klassifizieren. Die räumliche Ausdehnung dieser Strukturen wurde in einer weiteren Karte dargestellt. Die Korrelation der Ergebnisse, dargestellt in den verschiedenen Karten, hat dazu beigetragen, das Verständnis der komplexen glaziologischen Situation im zentralen Teil des Filchner-Ronne-Schelfeises zu verbessern. Darüber hinaus bietet das umfassende Datennetz eine vernünftige Basis zur weiteren Modellierung eines zweigeschichteten Schelfeises.

INTRODUCTION

The central part of Filchner-Ronne Ice Shelf (FRIS), Antarctica, includes a large area of about 150,000 km². The Institute Ice Stream forms the north-west boundary, while Korff Ice Rise, the Doake Ice Rumples and Henry Ice Rise mark the south-west boundary of the area. Its eastern boundary, as it is presented in this paper, is formed by Berkner Island.

For about ten years German scientists have intensively investigated the central part of FRIS. A main emphasis of the investigations was put on the description of the special glaciological situation of this region. Due to the spatial size of the observation region it was rational to carry out a program of airborne measurements and to develop a suitable instrumentation in order to obtain glaciological data all over the area in short time periods.

During the 1983/84 field season airborne electromagnetic reflection (EMR) measurements of the central part of FRIS were carried out within a long term project of the first author of this paper. The results of these measurements showed for the first time a clear double layering of the ice shelf. In an area close to the ice shelf edge the thickness of both layers, a meteoric ice layer and a marine ice layer, could be directly measured (THYSSEN 1985, 1988). During a second expedition, 1985/86, further airborne EMR measurements were carried out up to the south-west end of the central part of FRIS. After the processing of the data of both expeditions a more precise idea of the shape of the marine ice layer was developed (THYSSEN 1988). Within the same project a predicted total ice thickness of 450 m was confirmed by hot water drilling at a location about 200 km north-east of Henry Ice Rise (ENGELHARDT & DETERMANN 1987). The values of the total ice thickness also corresponded well with the results of earlier Russian measurements (POZ-DEYEV & KURININ 1987).

Since 1985/86 the idea of the existence of marine ice within the area of the central part of FRIS, suspected by ROBIN et al. (1983), has been accepted. Both layers, the meteoric ice layer formed by accumulated snow and the marine ice layer, which is formed by ice crystals frozen in the ocean water, have been clearly distinguished.

In the meantime a core has been drilled close to the ice shelf edge of the central part of FRIS, so that at present many isotopic and chemical data of the marine ice are additionally known (OERTER et al. 1992). In connection with this, the small salinity of the marine ice layer has been proved, i.e. the results of the core drilling corroborate the theory that this ice layer has a marine character rather than the saline character assumed previously.

As the flight tracks of the expeditions in 1983/84 and 1985/86 were in large areas, especially in the south central part of FRIS, not close enough, the exact boundary and thickness of the marine ice layer could not be determined with the desired accuracy. Therefore, during the 1989/90 field season an additional measuring program was carried out to investigate the shape of the marine ice layer in further detail.

In this paper results of all three expeditions are included. Figure 1 shows a map of the flight tracks forming the base of these results. In the following an improved surface elevation map, more detailed ice thickness maps of the different ice layers and

* Prof. Dr. Franz Thyssen, Andreas Bombosch and Henner Sandhäger, Forschungsstelle für physikalische Glaziologie, Universität Münster, Corrensstrasse 24, D-48149 Münster, FRG.

Manuscript received 16 December 1992; accepted 12 February 1993.

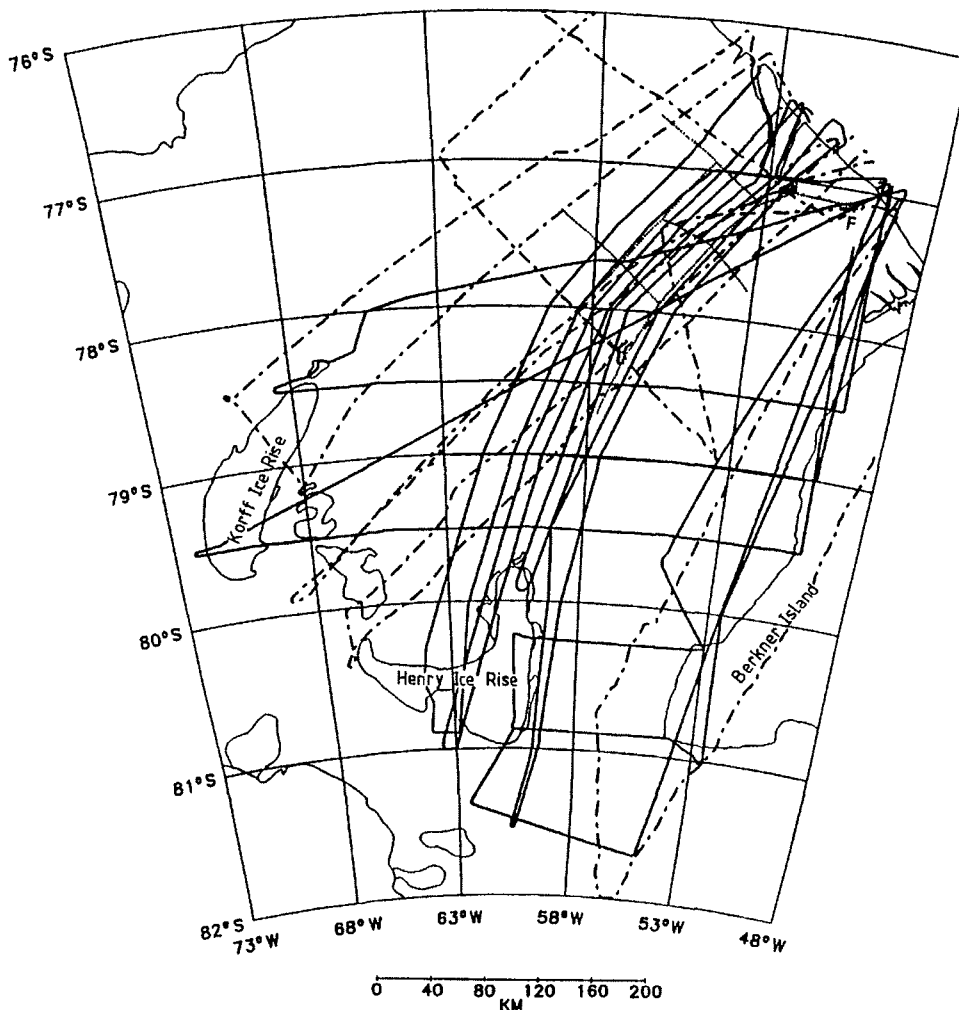


Fig. 1: Map of flight tracks on the central part of FRIS upon which results presented in this paper are based. Flight tracks from 1985/86 field season are plotted in dashed lines, flight tracks from 1989/90 field season in solid lines; the oversnow traverse (BLINDOW, RITTER & KARSTEN, pers. comm.) is plotted with the dotted line. Grounding lines, ice walls, significant topographic structures and ice front extracted from SWITHINBANK et al. (1988).

Abb. 1: Flugrouten der Meßflüge im zentralen Teil des FRIS, auf denen die Daten, die den hier vorgestellten Ergebnissen zugrunde liegen, gewonnen wurden. Flugrouten der Meßsaison 1985/86 sind mit strichpunktierten Linien, die der Saison 1989/90 mit durchgezogenen Linien dargestellt. Der Verlauf der Bodentrasverse (BLINDOW, RITTER & KARSTEN, pers. Mitteil.) ist durch die punktierte Linie gekennzeichnet. Aufsetzlinien, ausgeprägte topographische Strukturen und Schelfeisfront aus SWITHINBANK et al. (1988).

a new structure mark map are presented. The surface elevation of the ice shelf and the thickness of the meteoric ice layer could be measured. The thickness of the marine ice layer, however, was for the most parts derived from the apparent isostatic anomaly (THYSSEN1988, THYSSEN & GROSFELD 1988). Assuming isostatic equilibrium, the apparent isostatic anomaly was derived from the difference between the ice shelf elevation measured and an elevation corresponding to the meteoric ice thickness. Thus, the evaluated marine ice thickness is an equivalent solid ice thickness which includes all ice slush particles increasing the buoyancy, even if they are not consolidated.

During the 1989/90 field season a higher resolution of the EMR measurements and a more dense data net of the central part of FRIS were achieved, so a new emphasis of investigation called structure mark analysis became practicable. Especially in the EMR records of the 1989/90 season it was possible to select and to classify structure marks corresponding to real structures with-

in the ice. The understanding of these structure marks provides additional information about the general ice shelf dynamics.

EQUIPMENT

The airborne EMR measurements of all three expeditions mentioned above were carried out with the aircraft *Polar 2*, which was equipped with a precision radar altimeter, a barometric altimeter and an electromagnetic reflection system especially developed for these expeditions. In the first two field seasons, 1983/84 and 1985/86, a Doppler navigation system supported by Omega data was used. During the 1989/90 season a more exact inertial navigation system was installed. An important requirement for an exact measurement was to fly with the aircraft on an almost constant barometric pressure level. If possible, at the beginning and at the end of each flight the precision radar altimeter and the barometric altimeter were calibrated over

the open ocean on sea level. The airborne EMR measurements were done at a mean frequency of 35 MHz. The electromagnetic reflection signals were most of the time recorded at a rate of 4/s with a digital on-line averaging. The actual navigation data set was recorded at a rate of 1/s or 10/s including the radar and barometric altimeter data.

DATA PROCESSING AND MAPPING

In connection with the processing of the data some additional information was used to control and, if necessary, to correct the results of the airborne measurements mentioned above. In particular, additional surface elevation data from the area of the over snow traverse shown in Figure 1 (RITTER & KARSTEN pers. comm.) helped to achieve a high accuracy of the data net of this region. Along the traverse also ground-based EMR measurements were carried out. The results of these measure-

ments (BLINDOW pers. comm.) improved the knowledge of the local ice dynamics and of the structures within the meteoric ice in detail. On the other hand, information from glaciological maps of morphological features was not used for any corrections. Thus, in the areas of high surface elevation gradients the final results are less exact, caused by a data net too coarse in these regions, e.g. in the region of the Doake Ice Rumples or of the south-west part of Berkner Island. Consequently, the maps shown in the following were only developed on the base of digital data by using a standard interpolation program. In connection with the international FRIS-program the data have also been combined with others to produce new maps of all Filchner-Ronne Ice Shelf.

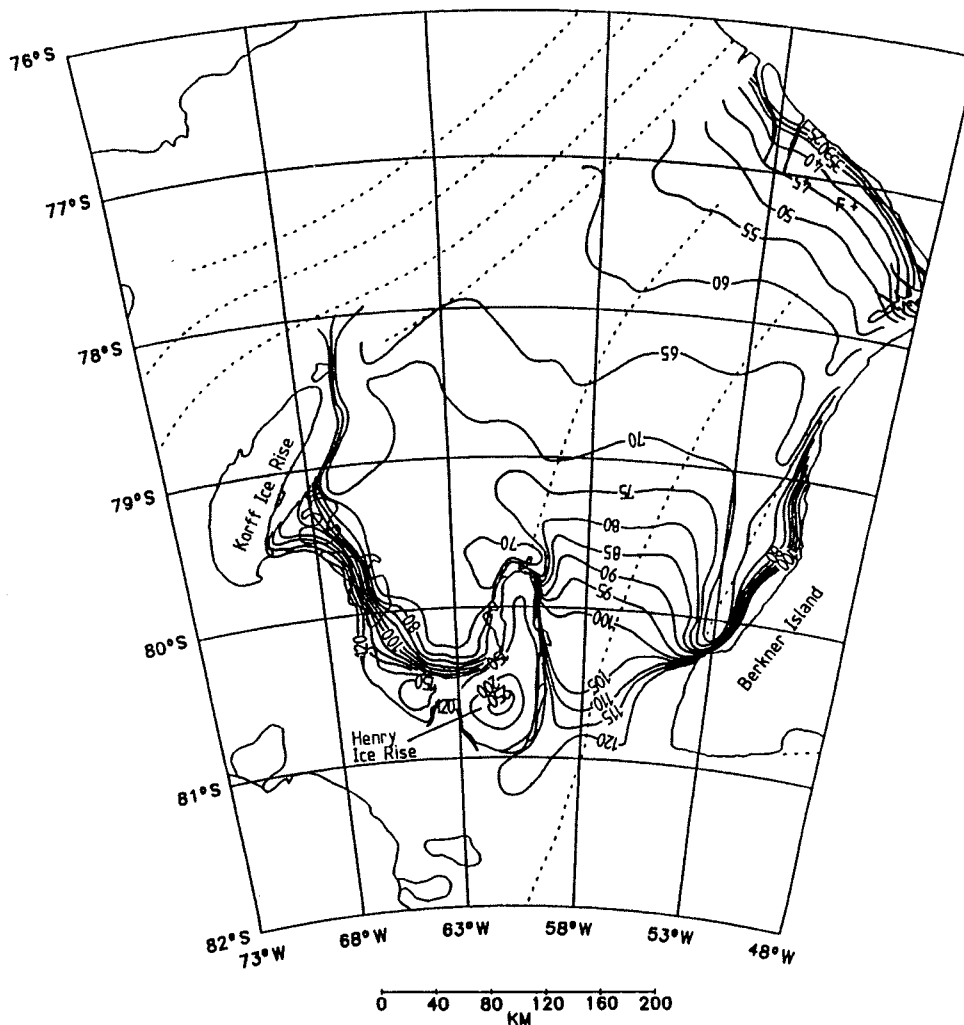


Fig. 2: Map of surface elevation of the central part of FRIS. Contour lines are plotted at intervals of 5 m with an accuracy estimated at ± 2 m. In areas of high surface elevation gradients the shape of the contour lines is less exact. Grounding lines, ice walls, significant topographic structures, ice front and ice stream margins extracted from SWITHINBANK et al. (1988).

Abb. 2: Freibordhöhen im zentralen Teil des FRIS. Die Höhenlinien sind in Intervallen von 5 m mit einer Genauigkeit von etwa ± 2 m dargestellt. In Gebieten großer Höhengradienten ist die Lage der Höhenlinien weniger sicher. Aufsetzlinien, ausgeprägte topographische Strukturen, Schelfeisfront und Eisstromgrenzen aus SWITHINBANK et al. (1988).

SURFACE ELEVATION AND TOTAL ICE THICKNESS

In the central part of FRIS isostatically balanced conditions exist almost everywhere, so the shape of the contour lines of the surface elevation map in Figure 2 and of the total ice thickness map in Figure 3 are very similar. For some parts, the total ice thickness values (i.e. the sum of the meteoric and marine ice thickness) were derived from the surface elevation data. The empirical formula used is published by THYSSEN (1988). The contour lines of the surface elevation map are plotted at intervals of 5 m. Apart from the data in the areas of high surface elevation gradients mentioned above, the accuracy of the elevation data is estimated at ± 2 m. On the other hand, the total ice thickness map shows contour lines plotted at intervals of 50 m. These results were determined with an estimated accuracy of ± 20 m. The contour lines of both maps suggest an ice damming process south of the Doake Ice Rumples, Henry Ice Rise and Berkner Island. Within the „channel“ between Henry Ice Rise and

Berkner Island the compression of the ice shelf is reduced. Especially north of this „channel“ the maps show a quick thinning of the ice shelf. The region at the northern end of Henry Ice Rise is additionally noticeable because of another complex morphology. This special situation is discussed later on in this paper.

ICE THICKNESS OF THE METEORIC AND THE MARINE ICE LAYER

In the central part of FRIS, two types of ice layers, the meteoric ice layer and the marine ice layer, are clearly distinguished. The maps of Figure 4 and Figure 5 show the thickness of these layers. The contour lines of both maps are plotted at intervals of 50 m. The accuracy of the data on the meteoric ice layer thickness is estimated at better than ± 10 m. The accuracy of the data on the marine ice layer thickness is estimated at ± 30 m.

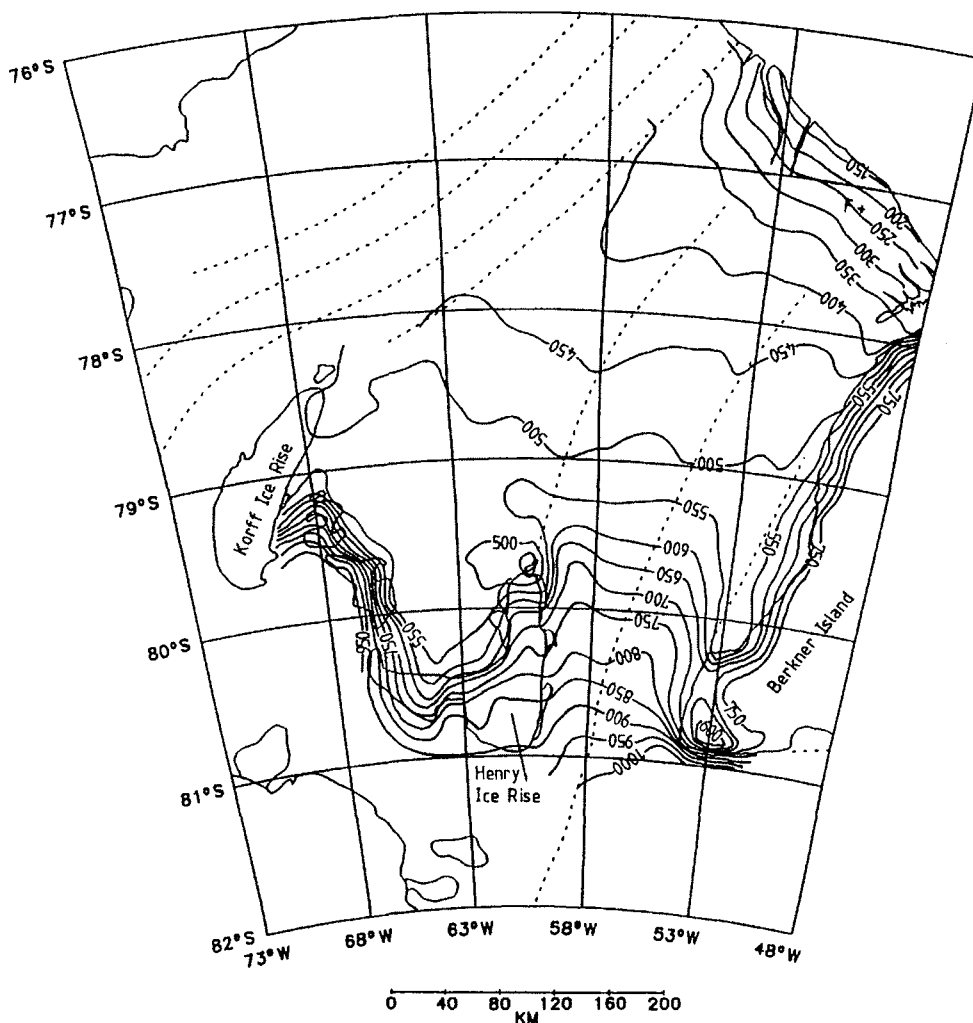


Fig. 3: Map of total ice thickness of central part of FRIS. Total ice thickness was derived both from the apparent isostatic anomaly and from direct measurements. Contour lines are plotted at intervals of 50 m with an accuracy of ± 20 m. Grounding lines, ice walls, significant topographic structures, ice front and ice stream margins extracted from SWITHINBANK et al. (1988).

Abb. 3: Gesamtmächtigkeit des Eises im zentralen Teil des FRIS. Die Gesamtmächtigkeit des Eises wurde zum Teil aus der scheinbaren isostatischen Anomalie berechnet und zum Teil durch direkte Messung ermittelt. Die Isolinien sind in Intervallen von 50 m mit einer Genauigkeit von etwa ± 20 m dargestellt. Aufsetzlinien, ausgeprägte topographische Strukturen, Schelfeisfront und Eisstromgrenzen aus SWITHINBANK et al. (1988).

The map of Figure 4 shows a well defined area with an unusually thin meteoric ice layer. The Institute Ice Stream forms the northwest boundary of this area, while Korff Ice Rise, the Doake Ice Rumples and Henry Ice Rise mark the south-west boundary of the area. Its eastern boundary corresponds to the boundary between Möller and Foundation Ice Stream. In the same area the marine ice layer is located, i.e. in the central part of FRIS marine ice only exists below a meteoric ice layer, which, on its own, would clearly not be in an isostatic equilibrium. The thickness of the marine ice layer is shown in the map of Figure 5. This map reveals a continuous thinning of the marine ice layer in the flow direction of the ice shelf. The layer disappears about 20-30 km from the ice shelf edge.

CLASSIFICATION AND MAPPING OF STRUCTURE MARKS

In connection with the structure mark analysis of the central part of FRIS, only those structure marks in the EMR records which corresponded to real structures within the meteoric ice were selected and classified. Structures within the marine ice would not have been completely resolved by the applied measuring technique anyway.

In general, it is possible to subdivide the selected structure marks into two groups: The first one includes reflections caused by layers within the meteoric ice. The second group discussed in the following includes diffraction hyperbolas having different forms of appearance. Further distinguishing criteria for the second group are the lateral density of occurrence of the hyperbolas and the vertical locations of their vertices in the EMR records. The diffraction hyperbolas are images of diffraction centres

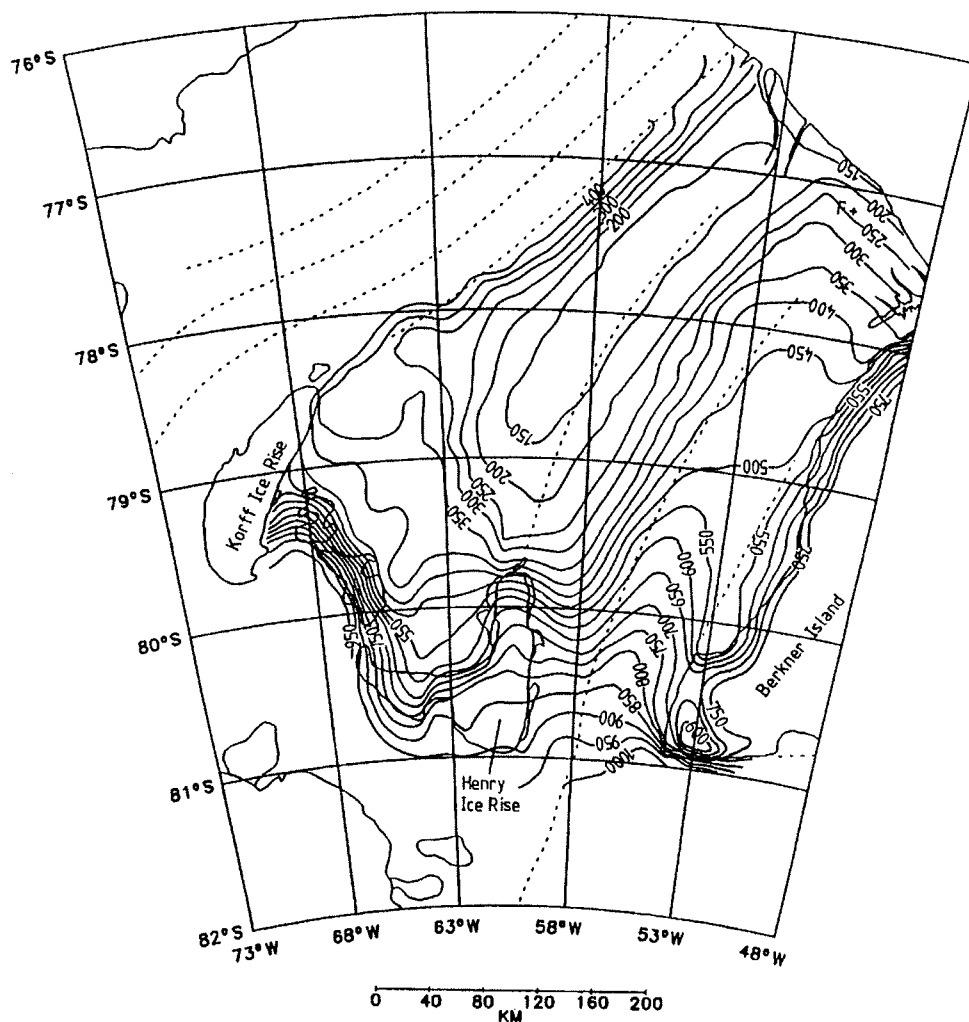


Fig. 4: Map of ice thickness of meteoric ice layer of central part of FRIS. The thickness of the meteoric ice layer could be directly measured. Contour lines are plotted at intervals of 50 m with an accuracy estimated at better than ± 10 m. Grounding lines, ice walls, significant topographic structures, ice front and ice stream margins extracted from SWITHINBANK et al. (1988).

Abb. 4: Mächtigkeit des meteorischen Eises im zentralen Teil des FRIS. Die Mächtigkeit wurde durch direkte Messung ermittelt. Die Isolinien sind in Intervallen von 50 m mit einer Genauigkeit von weniger als ± 10 m dargestellt. Aufsetzlinien, ausgeprägte topographische Strukturen, Schelfeisfront und Eisstromgrenzen aus SWITHINBANK et al. (1988).

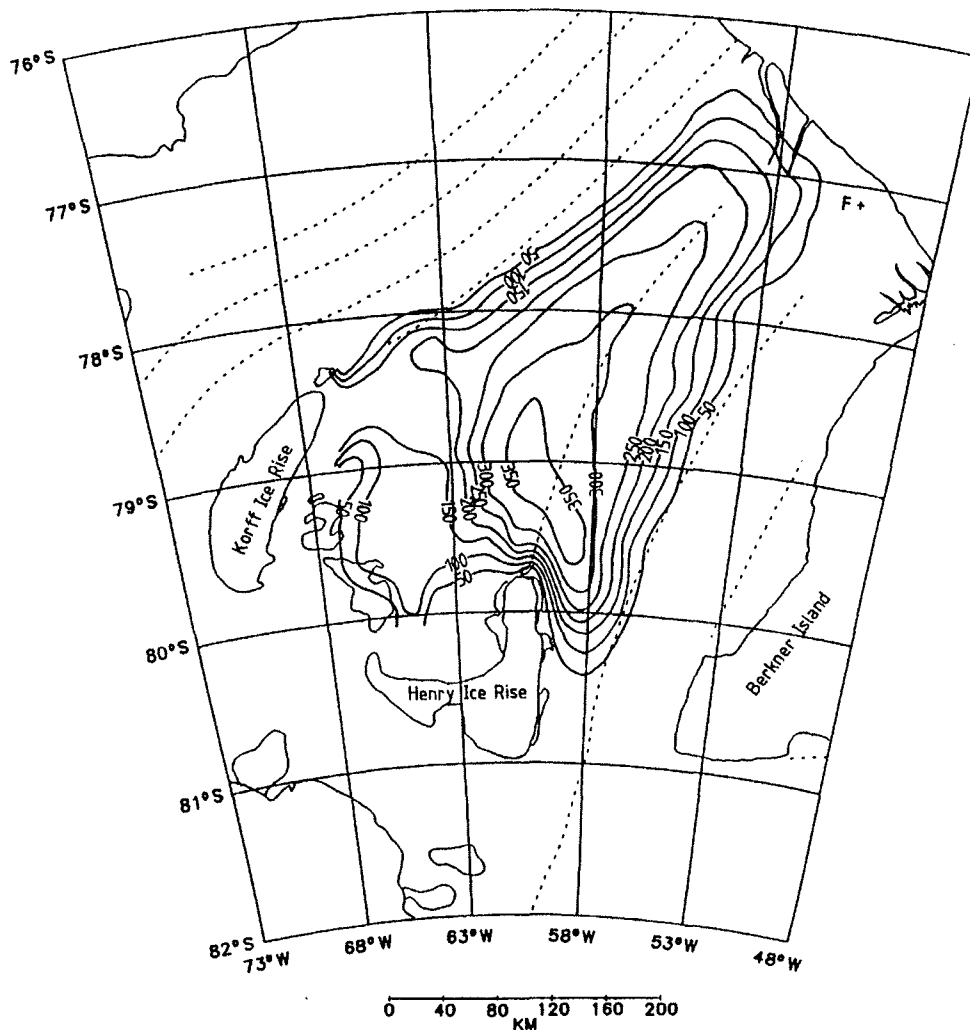


Fig. 5: Map of ice thickness of marine ice layer of central part of FRIS. Thickness of the marine ice layer was for most parts derived from the apparent isostatic anomaly. Contour lines are plotted at intervals of 50 m with an accuracy estimated at ± 30 m. Grounding lines, ice walls, significant topographic structures, ice front and ice stream margins extracted from SWITHINBANK et al. (1988).

Abb. 5: Mächtigkeit des marinen Eises im zentralen Teil des FRIS. Die Mächtigkeit wurde fast im gesamten Meßgebiet aus der scheinbaren isostatischen Anomalie berechnet. Die Isolinien sind in Intervallen von 50 m mit einer Genauigkeit von etwa ± 30 m dargestellt. Aufsetzlinien, ausgeprägte topographische Strukturen, Schelfeisfront und Eisstromgrenzen aus SWITHINBANK et al. (1988).

spatially assigned to the meteoric ice and its margins. These centres, on the whole, are causally related with crevasses and grooves of different dimensions and fillings.

Four fundamental classes of structure marks were selected, which will be shortly described and illustrated by examples showing their typical appearances:

The first class includes diffraction hyperbolas, whose vertices are located just below the dominant reflection from the ice shelf surface. In most cases the hyperbolas are clearly developed and are separated from each other. They can be identified as surface crevasses. Figure 6a (obtained about 50 km north-east of Henry Ice Rise) shows these structure marks in a typical EMR section. Since the upper part of the meteoric ice layer is not resolved in the EMR records, owing to an overmodulation of the amplifier used, it is usually difficult to determine the kind and the extent of the filling of the surface crevasses from an inspection

of the records. It needs further information to solve this problem.

Other diffraction hyperbolas, however, have their vertices located near the dominant reflection from the bottom of the meteoric ice layer. These hyperbolas are less clearly developed, but still separated from each other. Nevertheless, they fall into two different classes. On the one hand, they are found in EMR records of areas where the existence of a solid marine ice layer is not proved, but the existence of a marine ice slush can not be completely excluded. In this case, the vertices of the hyperbolas appear right above the reflection from the meteoric ice / sea water interface (see Fig. 6b, obtained in the basin north-west of Henry Ice Rise). The corresponding crevasses or grooves at the bottom of the meteoric ice layer are assumed to be filled with sea water. On the other hand, similar hyperbolas are found in records from areas where a marine ice layer definitely exists. In that case, the vertices of the hyperbolas are located near the

reflection from the meteoric / marine ice interface (see Fig. 6c, obtained about 100 km north-west of Henry Ice Rise). In these regions of FRIS former crevasses or grooves at the bottom of the meteoric ice layer are sealed in by marine ice. They are conserved until the whole marine ice layer has melted.

The fourth class of the selected structure marks includes reflection signals which are almost randomly distributed. The signals are spread out over the whole area underneath the dominant reflection from the ice shelf surface.

In several EMR records, reflection signals of the same type, but

more widely separated, can be identified as a number of diffraction hyperbolas. Further on in these records, the hyperbolas overlap more and more. That is why this structure mark is called „diffraction noise“. It is caused by fragmentarily destroyed meteoric ice, which randomly diffracts the electromagnetic waves penetrating the ice shelf.

A progressive transition from the „diffraction noise“ to separated diffraction hyperbolas, interpreted as surface crevasses, is typical for the distribution of structure marks within the EMR records of the central part of FRIS. The delimitation of these structure marks is difficult. Therefore, in the structure mark

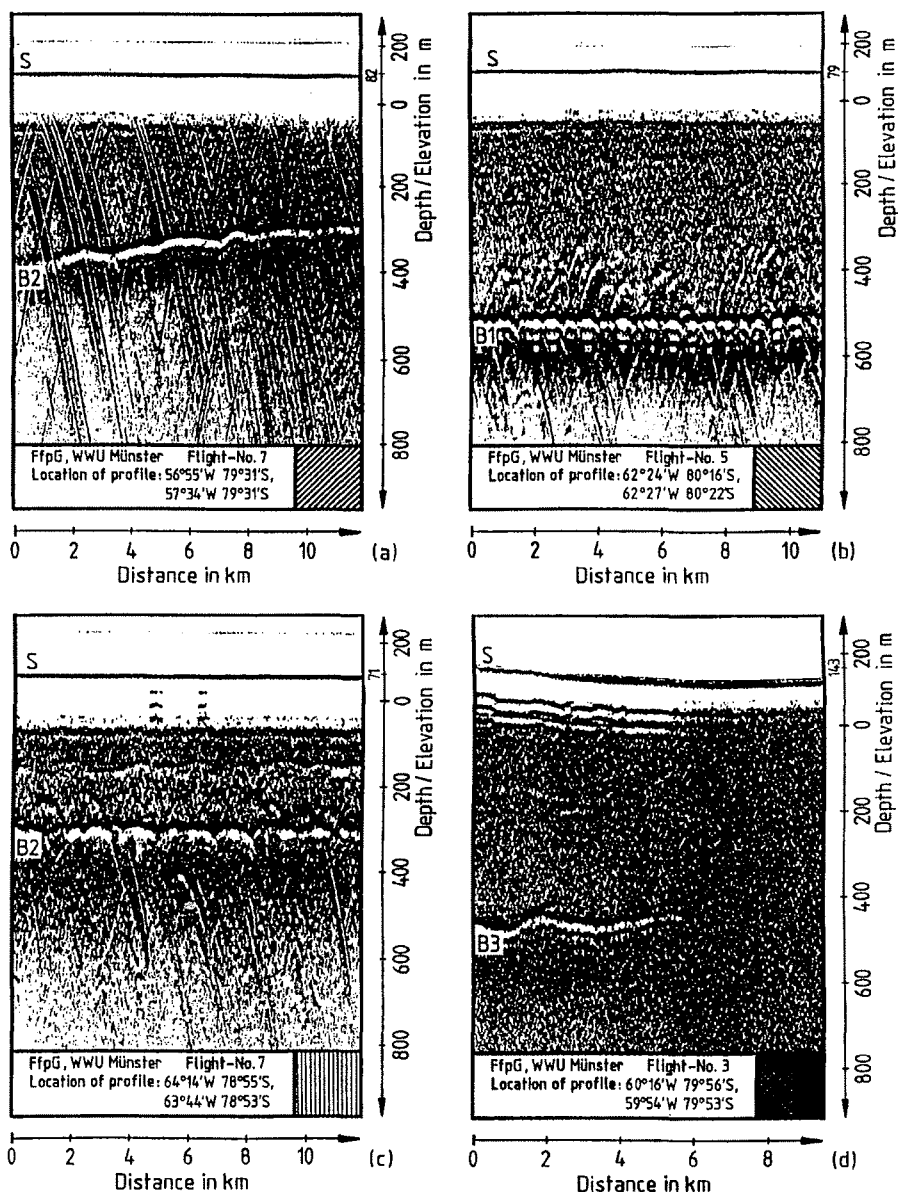


Fig. 6: EMR sections showing examples of the selected structure marks.

- (a) EMR section showing diffraction hyperbolas, whose vertices are located just below the reflection from the ice surface S;
- (b) EMR section showing diffraction hyperbolas, whose vertices are located right above the reflection from the meteoric ice / sea water interface B1.
- (c) EMR section showing diffraction hyperbolas, whose vertices are located near the reflection from the meteoric / marine ice interface B2.
- (d) EMR section showing the two types of „diffraction noise“. In the left part of the section the reflection from the bottom of the meteoric ice layer, which, in this case, corresponds with the meteoric ice / bed rock interface B3, can be seen. In the right part the reflector is obscured.

Abb. 6: EMR-Registrierungen mit Beispielen für die ausgewählten Strukturmerkmale.

analysis presented two types of „diffraction noise“ are distinguished, the second of which represents the transition to separated hyperbolas. In the EMR records of the first type the „diffraction noise“ is so strong that the reflection from the bottom of the meteoric ice layer is obscured, i.e. the meteoric ice is destroyed. In the records of the second type the bottom reflection can be seen through the „diffraction noise“. Figure 6c (obtained at the north end of Henry Ice Rise) shows an EMR section with both types of „diffraction noise“.

The final result of the structure mark analysis described above is the structure mark map shown in Figure 8. The regions characterized by different structure marks were determined by interpolation.

The crevasses at the bottom of the meteoric ice layer, which are sealed in by marine ice, are spread out over a well defined area. The boundaries of this area correspond almost exactly to the boundaries of the marine ice layer mentioned above, i.e. sealed crevasses at the bottom of the meteoric ice can be found wherever the existence of the marine ice layer is proved. In a part of this area, north of Henry Ice Rise, other structures within the meteoric ice are dominant. A region of fragmentarily destroyed meteoric ice is surrounded by a region of surface crevasses. The typical progressive transition zone described above exists in between. The structures are arranged in a distinctive pattern which has been deformed by the general ice shelf flow.

LINEAR ARRANGED STRUCTURES AT THE METEORIC / MARINE ICE INTERFACE

In addition to the classified structure marks described above another type of structure, shown in Figure 7, can be found in several EMR records. These structure marks, groups of deformed and almost parallel reflection horizons, are for the most part caused by side reflections from linearly arranged crevasses or grooves, called in the following „linear elements“, at the bottom of the meteoric ice layer. These elements are orientated in the direction of the local ice shelf flow.

In order to receive the side reflections from the „linear elements“, an antenna system had to be used for the airborne measurements which had a measuring characteristic most sensitive in the direction perpendicular to the line of flight. During the measuring process, whenever the aircraft flew almost parallel to the „linear elements“ at the meteoric / marine ice interface (see Fig. 8) structure marks as shown in Figure 7 appeared in the EMR records, i.e. during the measuring process an immediate structure mark analysis can be used to determine the direction of the local ice shelf flow. Further investigations of this structure mark analysis are planned.

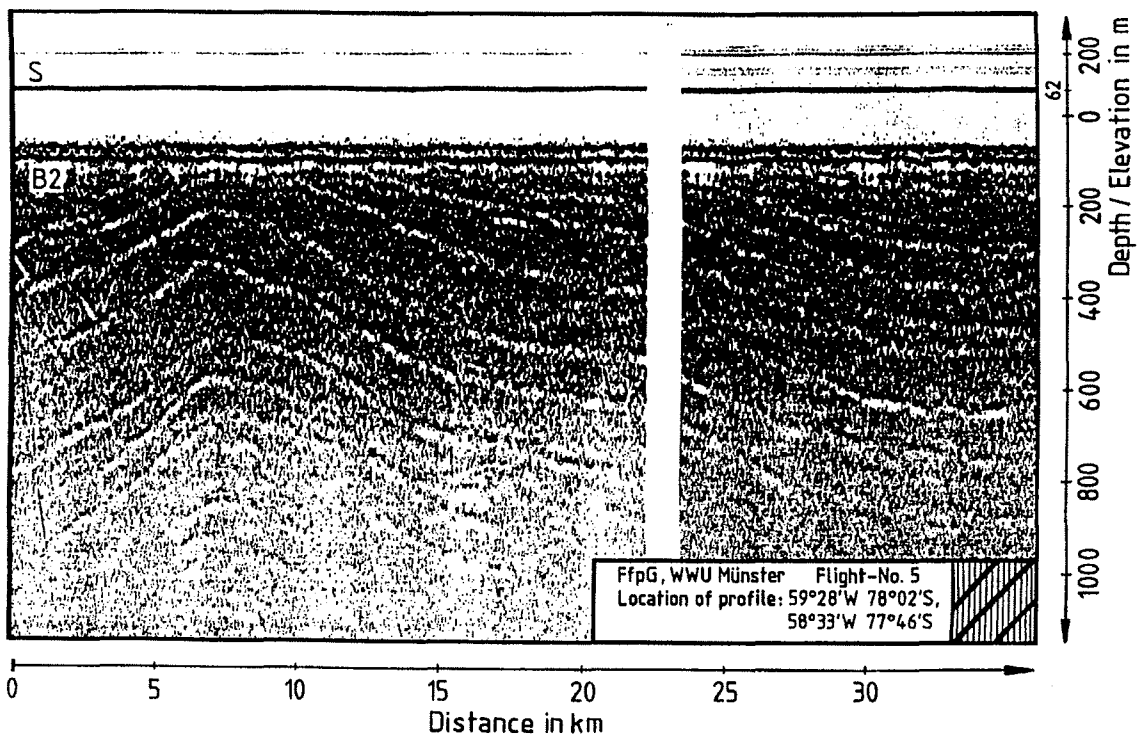


Fig. 7: EMR section showing an example of the structure mark assumed to be caused by side reflections of the electromagnetic waves from several „linear elements“ at the meteoric / marine ice interface (B2). During the measuring process the aircraft flew almost parallel to the „linear elements“.

Abb. 7: EMR-Registrierung als Beispiel für das Strukturmerkmal, das auf Seitenreflektionen der elektromagnetischen Wellen an einigen „linearen Elementen“ im Bereich der Grenzschicht zwischen meteorischem und marinem Eis (B2) zurückgeführt werden kann. Während der Messung wurde annähernd parallel zu den „linearen Elementen“ geflogen.

CONCLUSION

The main emphasis of the three expeditions mentioned was put on the description of the glaciological situation within the area of the marine ice layer. Thus, the glaciological situations of the surrounding areas, such as the region of Foundation Ice Stream and of Berkner Island, are not discussed in this paper.

The different maps presented of the central part of FRIS show detailed information about the surface elevation, the total ice thickness, the thickness of the two ice layers and the structures within the ice. In the future this information can be used as a base for ice shelf modelling.

Comparing all maps of the paper, a correlation of the results can be observed. In this connection an area north of Henry Ice Rise is clearly noticeable owing to the complex glaciological conditions there. The meteoric ice layer of this area is fragmentarily

destroyed. In good agreement, the glaciological map of FRIS (SWITHINBANK 1988) shows corresponding features on the ice shelf surface in this region. The formation of these structures on and within the ice shelf is assumed to be connected with the formation process of the marine ice layer. The map of the surface elevation of FRIS reveals a low ridge about 100 km long, north-east of Henry Ice Rise, which ends in the area described. As the maximum thickness of the marine ice layer is located in the same area north of Henry Ice Rise, the basic formation process of the marine ice seems to be reduced north of this region.

If this is the case, the existence of the marine ice below the meteoric ice layer close to the ice shelf edge must be caused by the movement of the ice shelf. The meteoric ice and the marine ice flow in the same direction towards the ice shelf edge until they have melted from the base or calved from the edge.

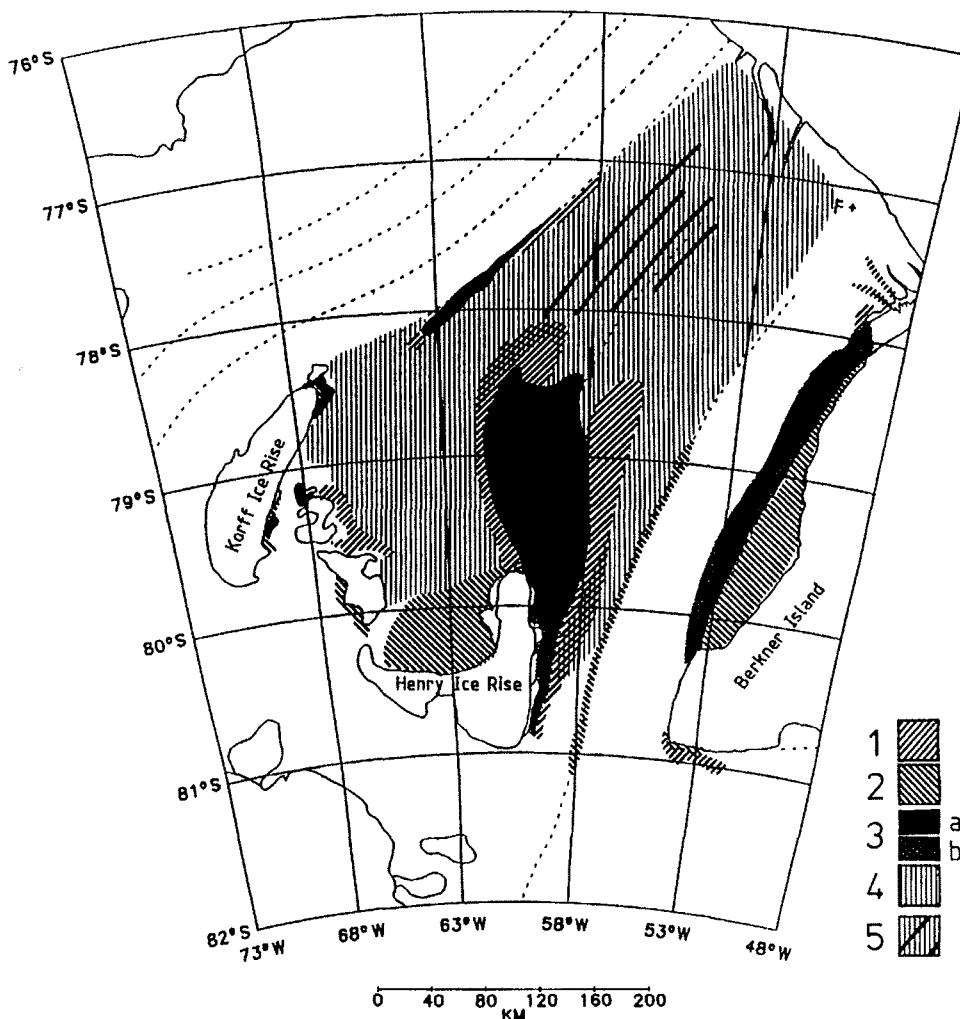


Fig. 8: Map of selected structure marks of the central part of FRIS. Grounding lines, ice walls, significant topographic structures, ice front and ice stream margins extracted from SWITHINBANK et al. (1988).

(1) surface crevasses; (2) crevasses or grooves at the bottom of the meteoric ice layer assumed to be filled with sea water; (3) fragmentarily destroyed meteoric ice, a: destroyed meteoric ice, b: less destroyed meteoric ice; (4) former crevasses or grooves at the bottom of the meteoric ice layer now sealed in by marine ice; (5) several parts of flight tracks running almost parallel to „linear elements“ at the meteoric / marine ice interface.

Abb. 8: Verbreitung der ausgewählten Strukturmerkmale im zentralen Teil des FRIS. Aufsetzlinien, ausgeprägte topographische Strukturen, Schelfeisfront und Eisstromgrenzen aus SWITHINBANK et al. (1988).

ACKNOWLEDGEMENTS

This work has been supported by the Bundesministerium für Forschung und Technologie, the Deutsche Forschungsgemeinschaft, the Ministerium für Wissenschaft und Forschung Nordrhein-Westfalen and the Alfred-Wegener-Institut für Polar- und Meeresforschung.

References

- Engelhardt, H. & Determann J.* (1987): Borehole evidence for a thick layer of basal ice in the central Ronne Ice Shelf.- *Nature* 327 (6120): 318-319.
- Oerter, H., Kipfstuhl J., Determann J., Müller H., Wagenbach D., Minikin A. & Graf W.* (1992): Evidence for basal marine ice in the Filchner-Ronne ice shelf.- *Nature* 358 (6385): 399-401.
- Pozdeyev, V.S. & Kurinin R.G.* (1987): New data on the morphology of the ice cover and relief of the subglacial bed and sea bottom in the southern part of the Wedell Sea basin (West Antarctica) (in Russian).- *Antarctica* 26: 66-71.
- Robin, G. de Q., Doake C.S.M., Kohnen H., Crabtree R.D., Jordan S.R. & Möller D.* (1983): Regime of the Filchner-Ronne ice shelves, Antarctica.- *Nature* 302 (5909): 582-586.
- Swithinbank, C., Brunk K. & Sievers J.* (1988): A glaciological map of Filchner-Ronne Ice Shelf, Antarctica. *Annals Glaciol.* 11: 150-155.
- Thyssen, F.* (1985): First results from Polar-2-measurements on the Filchner and Ekström ice shelves.- In: H. Kohnen (ed.), *Filchner-Ronne-Ice-Shelf-Programme Report No. 2.*, Bremerhaven, Alfred-Wegener-Institute, 131-132.
- Thyssen, F.* (1988): Special aspects of the central part of Filchner-Ronne Ice Shelf, Antarctica- *Annals Glaciol.* 11: 173-179.
- Thyssen, F. & Grosfeld K.* (1988). Ekström Ice Shelf, Antarctica.- *Annals Glaciol.* 11: 180-183.